Dust attenuation in galaxies up to redshift similar or equal to 2

V. Buat

Earth Planets Space, **65**, 1095–1100, 2013

Dust attenuation in galaxies up to redshift $\simeq 2$

V. Buat

Aix-Marseille Université, CNRS, LAM (Laboratoire d'Astrophysique de Marseille) UMR7326, 13388, France

(Received October 25, 2012; Revised January 17, 2013; Accepted February 2, 2013; Online published October 24, 2013)

We want to study dust attenuation at ultraviolet (UV) wavelengths at high redshift, where the UV is redshifted to the observed visible light wavelength range. In particular, we search for a bump at 2175 Å. We use photometric data in the *Chandra* Deep Field South (CDFS), obtained in intermediate and broad band filters by the MUSYC project, to sample the UV rest-frame of 751 galaxies with $0.95 < z < 2.2$. When available, infrared (IR) *Herschel*/PACS* data from the GOODS-*Herschel* project, coupled with *Spitzer*/MIPS measurements, are used to estimate the dust emission and to constrain dust attenuation. The spectral energy distribution of each source is fit using the CIGALE code†. The average attenuation curve found for our sample galaxies exhibits a UV bump whose amplitude is similar to that observed in the extinction curve of the LMC super-shell region. The slope of the average attenuation curve at UV wavelength is found steeper than that for local starburst galaxies. The amount of dust attenuation at UV wavelengths is found to increase with stellar mass and to decrease as UV luminosity increases.

Key words: Galaxies: high-redshift, galaxies: ISM, ultraviolet:galaxies, dust: extinction.

1. Introduction

Although dust is a minor component in galaxies, it captures a large fraction of the stellar emission, especially at short wavelengths. This process makes the direct observation of stellar populations from the UV to the near-IR insufficient to recover all the emitted photons. Thus reliable dust corrections are mandatory for measuring the star formation rate (SFR) in the universe and its evolution with redshift from UV-optical surveys. The search for relations between dust attenuation and observed or commonly measured quantities are very useful in this context. It is also particularly important to study the dependence of dust attenuation on wavelength in order to recover the intrinsic spectral distribution of the stellar light, which gives information on the star formation history at work in galaxies.

Models solving radiation transfer rely on numerous free parameters and physical assumptions that are difficult to constrain from the integrated emission from entire galaxies and for very large numbers of objects. Simpler models have been specifically developed to analyze large samples of galaxies, introducing simple recipes and templates. The number of free parameters is considerably reduced. These codes are often developed to measure photometric redshifts and physical parameters such as the SFR and the stellar mass. With the availability of mid and far-IR data for large samples of galaxies, new codes are emerging that combine stellar and dust emission on the basis of the balance between the stellar luminosity absorbed by dust and the corresponding luminosity re-emitted in the IR. Attenuation laws are introduced in these codes. The most popular attenuation curve is that of Calzetti *et al*. (2000), built for local starburst galaxies. This law, based on spectroscopic data, does not exhibit a bump at 2175 Å such as that observed in the extinction curves of the Milky Way (MW) or the Large Magellanic Cloud supershell (LMC2). Since the Calzetti and collaborators work, numerous studies have tried to search for the presence of a bump in the attenuation curve of nearby, non starbursting, galaxies. Most studies based on very different approaches conclude to a presence of bump in large samples of nearby star forming galaxies (Burgarella *et al*., 2005; Conroy *et al*., 2010; Wild *et al*., 2011). At higher redshifts, the situation is more favorable because of the redshifting of the UV emission into visible. Direct evidence of bumps came from the analysis of the galaxy spectra at $1 < z < 2.5$ (Noll *et al*., 2009). Recently Buat *et al*. (2011b, 2012) analyzed spectral energy distributions (SEDs) of UV selected galaxies in a redshift range between 0.95 and 2.2, observed through intermediate band filters and with IR detections from *Herschel*/PACS, and found evidence for a UV bump in the dust attenuation curve of all these galaxies. The present work extends the analysis performed in these two papers. After a brief description of the data (Section 2) and of the fitting tool used for the analysis (Section 3), the average attenuation curve obtained with the dataset is compared to extinction curves of LMC2 and MW and to the models of Inoue *et al*. (2006) in Section 4. Relations linking dust attenuation to UV luminosity and stellar mass are presented in Section 5.

Herschel is an ESA space observatory with science instruments provided by European-led Principal Investigator consortia and with important participation from NASA.

†cigale.oamp.fr

doi:10.5047/eps.2013.02.001

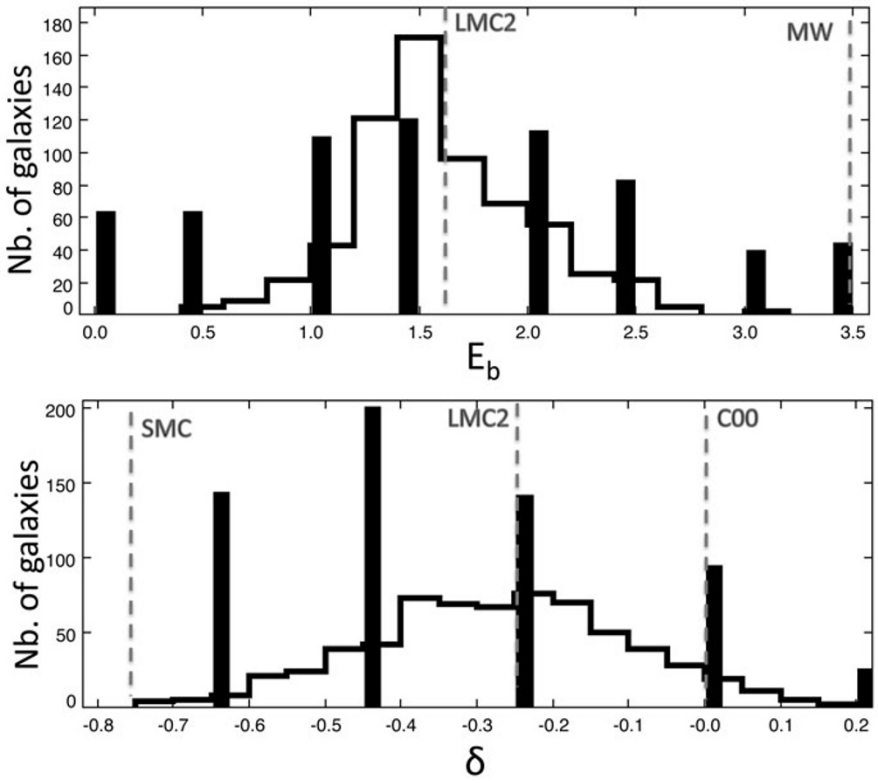

Fig. 1. Distribution of the amplitude of the bump E_b and slope of the attenuation curve δ as defined in Eq. (1) and (2). Both parameters are determined with the CIGALE code which does not only give the best model fitted (based on a χ^2 minimization over all the models) but also calculates the probability of each input model and returns the probability distribution function (PDF) of each parameter. The histograms with spikes correspond to the values found for the best models and the continuous lines represent the distributions of the mean values of the PDF of E_b and δ obtained for each object. The values corresponding to the attenuation curve of Calzetti *et al.* (2000, C00), of the extinction curves of the Milky Way (MW), LMC2 supershell (LMC2) and of the SMC (SMC) are plotted as dotted lines. The parameters for the MW are taken from Fitzpatrick and Massa (1990), those for the Magellanic Clouds come from Gordon *et al.* (2003).

2. High Redshift Galaxies Selected in the Ultraviolet

The sample selection is described in Buat *et al.* (2012). We briefly summarize the selection process and the main characteristics of the resulting sample. The field considered is located in the Great Observatories Origins Deep Survey Southern field (GOODS-S). It was observed at 100 and 160 μm over 264 hours by the PACS instrument onboard of the *Herschel* Space Observatory (Pilbratt *et al.*, 2010) as part of the GOODS-*Herschel* open time key project (Elbaz *et al.*, 2011). The MUSYC project (Cardamone *et al.*, 2010) compiled a uniform catalogue of optical and IR photometry for sources in this field, incorporating the GOODS *Spitzer* IRAC and MIPS data as well as intermediate and broad-band optical data. It provides a valuable means of tracing the detailed shape of the UV rest-frame spectrum. We started with the MUSYC catalogue, selecting sources with a spectroscopic redshift between 0.95 and 2.2 and no X ray detection. In this redshift range we have more than ten photometric bands available in the UV rest-frame and a good sampling around 2175 Å. We consider all the optical broad bands (7 bands from U to z) and intermediate-band filters (11 bands) whose $5\,\sigma$ depth was fainter than 25 ABmag. Our sample contains 751 sources, all detected by IRAC at 3.6 μm. 290 sources have a $3\,\sigma$ detection at 24 μm, 76 of these sources are also detected by PACS at 100 μm.

3. CIGALE: A SED Fitting Tool Aimed at Studying Dust Attenuation in Galaxies

The CIGALE code (Code Investigating GALaxy Emission, http://cigale.oamp.fr) was developed by Noll *et al.* (2009). This is a physically-motivated code that derives properties of galaxies by fitting their UV-to-IR SEDs. CIGALE combines a UV-optical stellar SED with a dust component emitting in the IR and fully conserves the energy balance between the dust absorbed stellar emission and its re-emission in the IR. We refer to Noll *et al.* paper for details on the code. For the purpose of the present work we focus on the dust attenuation treatment performed by CIGALE, the various input parameters introduced for this analysis are discussed in Buat *et al.* (2012). The dust attenuation is described as

$$A(\lambda) = \frac{A_V}{4.05}\,(k'(\lambda) + D_{\lambda_0,\gamma,E_b}(\lambda))\left(\frac{\lambda}{\lambda_V}\right)^{\delta}, \qquad (1)$$

Throughout the paper the wavelength λ will be expressed in Å, $\lambda_V = 5500$ Å, $k'(\lambda)$[1] comes from Calzetti *et al.* (2000) (Eq. (4)) and $D_{\lambda_0,\gamma,E_b}(\lambda)$, the Lorentzian-like Drude profile

[1] $k'(\lambda) = 2.659(-2.156 + 1.50910^4/\lambda - 0.19810^8/\lambda^2 + 0.01110^{12}/\lambda^3) + 4.05$ for $1200 < \lambda < 6300$ Åand $k'(\lambda) = 2.659(-1.857 + 1.04010^4/\lambda) + 4.05$ for $6300 < \lambda < 22000$ Å

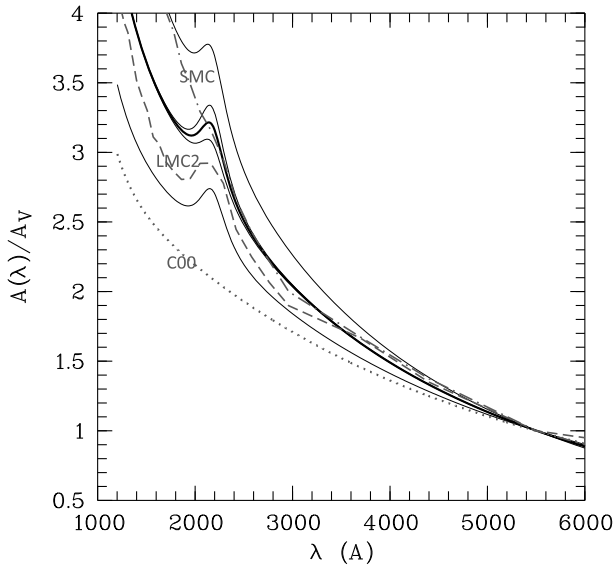

Fig. 2. Mean dust attenuation curve (black heavy line), the thin black lines represent the 1 σ variation on E_b and δ. The attenuation curve of Calzetti (2000) is plotted as a dotted line (C00), the LMC2 extinction curve with a dashed line and the SMC extinction curve with a dot-dashed line.

commonly used to describe the UV bump, is defined as

$$D_{\lambda_0,\gamma,E_\mathrm{b}} = \frac{E_\mathrm{b}\lambda^2\gamma^2}{(\lambda^2-\lambda_0^2)^2+\lambda^2\gamma^2}. \quad (2)$$

The factor $\left(\frac{\lambda}{\lambda_\mathrm{V}}\right)^\delta$ produces different slopes without modifying the visual attenuation A_V. It implies changes in the value of the effective total obscuration R_V, originally equal to 4.05 for the Calzetti *et al*. law.

The reliability of parameter determinations is extensively discussed in Buat *et al*. (2012) with the analysis of a catalog of artificial galaxies and that of the 76 galaxies detected by PACS. Parameters are better estimated when at least one IR measurement is available, which is the case for 290 of our objects. Without IR data dust attenuation at UV wavelength is found slightly over-estimated for low values of this parameter (of the order of 0.3 mag for an attenuation of 1 mag), the amplitude of the bump E_b is robustly estimated whereas the slope δ is over-estimated for low values (by 0.1 unit for $\delta = -0.5$). We refer to Buat *et al*. (2012) for more details about the SED fitting analysis.

E_b and δ are estimated for each object as the mean value of their probability distribution function (PDF) given by CIGALE. The resulting distributions obtained for these estimated parameters are shown in Fig. 1. The typical uncertainty for each estimation (dispersion of the PDF) is found to be 0.8 for E_b and 0.15 for δ. The average values and standard deviations of the distributions of Fig. 1 are $\langle E_\mathrm{b}\rangle = 1.6 \pm 0.4$ and $\langle\delta\rangle = -0.27 \pm 0.17$. The large uncertainty in the determination of the parameters implies that only 20% of individual sources (40% of the sources detected in IR) exhibit a secure bump and and an attenuation curve steeper than the Calzetti *et al*. one. In the next section, we will focus on the analysis of the average attenuation curve and not on the dispersion found for individual source. A detailed discussion of the individual measurements can be found in Buat *et al*. (2012).

4. Average Dust Attenuation Curve

We can tentatively derive an average attenuation curve for our sample.

$$\frac{A(\lambda)}{A_\mathrm{V}} = \frac{k'(\lambda)+D_{\lambda_0,\gamma,E_\mathrm{b}}(\lambda)}{4.05}\left(\frac{\lambda}{\lambda_\mathrm{V}}\right)^{-0.27} \quad (3)$$

with

$$D_{\lambda_0,\gamma,E_\mathrm{b}}(\lambda) = \frac{1.6\times 350^2\lambda^2}{(\lambda^2-2175^2)^2+\lambda^2\times 350^2} \quad (4)$$

Models predict a variation of the shape of the attenuation curve and of the amplitude of the bump with the amount of dust attenuation (e.g. Inoue *et al*., 2006). The mean dust attenuation at 1530 Å for the sample is found to be $\langle A_\mathrm{FUV}\rangle = 2.2$ mag and the average dust attenuation curve given above is expected to be representative of galaxies with this average attenuation.

The resulting curve is plotted in Fig. 2 with other curves already considered in Fig. 1. As underlined in Buat *et al*. (2012) the average attenuation curve is close to the extinction curve found for the LMC2 super-shell. Inoue *et al*. (2006) predicted various attenuation curves for the UV range. In Fig. 3 we compare the result of their models obtained with dust characteristics from Draine (2003) and corresponding to $A_\mathrm{FUV} = 2$ mag. The extinction curve for the LMC2 super-shell is also over-plotted. Whereas the amplitude of the bump is well reproduced in the Inoue *et al*. model with LMC dust, the corresponding attenuation curve is steeper than the one derived from the data. The general shape is better reproduced with a MW type dust but this time the predicted amplitude of the bump is too large. The best agreement is found with the LMC2 extinction curve.

5. Dust Attenuation Variation

In the absence of IR emission to constrain dust attenuation, empirical relations linking the amount of dust attenuation to some galaxy characteristics are particularly use-

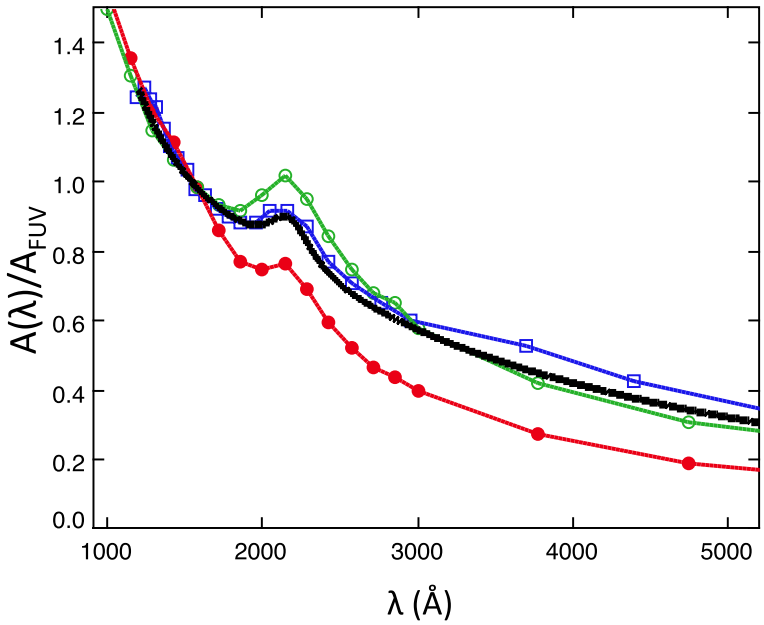

Fig. 3. Average dust attenuation curve derived in this work (black solid line) compared to models from Inoue *et al*. for a LMC2 type dust (filled circles and red line), and a MW type dust (empty circles and green line). The empty squares and blue line are for the LMC2 extinction curve from Gordon *et al*. (2003).

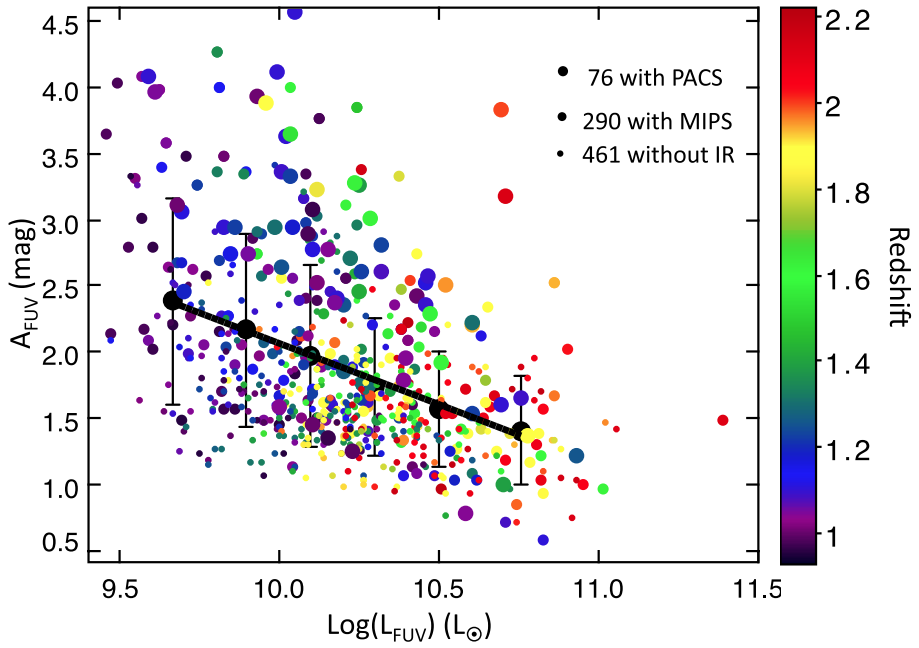

Fig. 4. Dust attenuation versus FUV luminosity. Redshift is color coded. The connected black points and the vertical bars represent the mean and dispersion of $A_{\rm FUV}$ per bin of $L_{\rm FUV}$. The solid line is the result of the linear regression.

ful. Any systematic trend with the observed UV luminosity is important to account for when intrinsic, attenuation corrected luminosity functions are studied. Another crucial physical parameter is the stellar mass. It is mainly constrained by the optical-NIR part of the SED which is not very sensitive to dust attenuation and can be securely estimated even when dust attenuation is badly known. As a consequence any relation between dust attenuation and stellar mass will be particularly useful at least to apply global corrections to large samples of galaxies. Hereafter we will discuss dust attenuation at FUV, with a FUV wavelength taken at 1530 Å (corresponding to the FUV GALEX filter). The FUV luminosity $L_{\rm FUV}$ is defined as $\lambda \times L_\lambda$ and expressed in solar units ($L_\odot$).

5.1 Dust attenuation and observed luminosities

Buat *et al*. (2012) (see also Heinis *et al*., *MNRAS*, submitted) reported a decrease of the mean dust attenuation when the observed FUV luminosity increases with a dispersion increasing at low luminosities. The data points and the average values per bin of FUV luminosity calculated by Buat

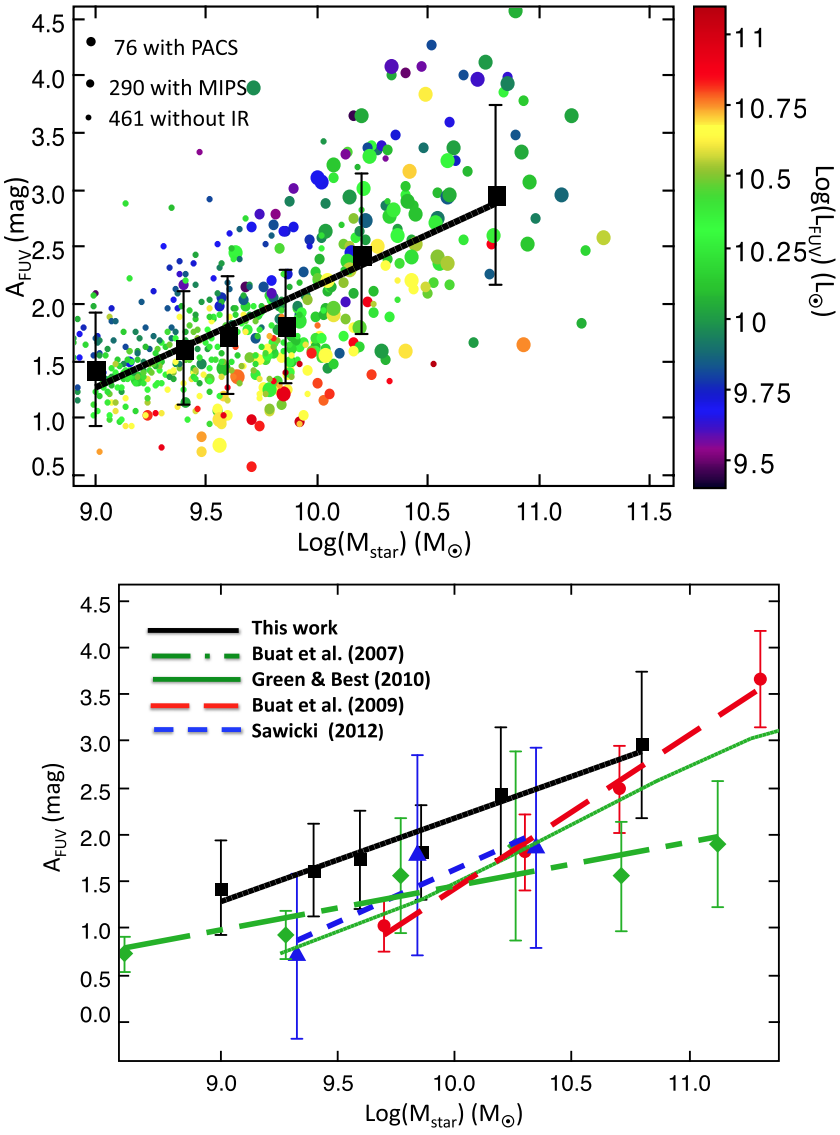

Fig. 5. Dust attenuation versus stellar mass. Upper panel: Individual values of $M_{\rm star}$ and $A_{\rm FUV}$ from Buat *et al.* (2012) are reported with the observed FUV luminosity color coded. The mean values and the related dispersion per bin of $M_{\rm star}$ from Buat *et al.* (2012) are plotted with filled squares and vertical bars. The solid line is the result of the linear regression. Lower panel: the linear regression found in the upper panel (filled squares and black lines) is compared with other relations from previous works: at $z = 0$ from Buat *et al.* (2007) (lozenges and green dot-dashed regression line) and from Garn and Best (2010) (solid thin green line), for $z < 1$ from Buat *et al.* (2009) (red dots and dashed line, average relation for $\langle \log(L_{\rm FUV}) = 10.2[L_\odot] \rangle$) and at $z = 2$ from Sawicki (2012) (blue dotted line and triangles).

et al. (2012) are reported in Fig. 4. We perform a linear regression between the average values of $A_{\rm FUV}$ expressed in magnitudes and $L_{\rm FUV}$ in solar units:

$$A_{\rm FUV} = (-0.93 \pm 0.04) \times \log(L_{\rm FUV}) + (11.33 \pm 0.45) \quad (5)$$

the uncertainties on the coefficients (slope and constant) correspond to standard deviations, the global R.M.S. error is found equal to 0.04, and the correlation coefficient R is equal to 0.99.

The detected galaxies become more luminous when the redshift increases because of selection effects as clearly seen in Fig. 4. So any study of the variation of dust attenuation with z must account for this decrease of the attenuation when $L_{\rm FUV}$ increases.

5.2 Dust attenuation and stellar masses

Stellar masses ($M_{\rm star}$) are obtained as an output of the fitting code CIGALE as described in Buat *et al.* (2012). The adopted IMF is that of Kroupa (2001). Mean dust attenuation factors can be calculated per bin of $M_{\rm star}$, the results are reported in Fig. 5. We perform a linear regression on these average values, the correlation coefficient is found very high ($R = 0.97$) and the linear regression gives:

$$A_{\rm FUV} = (0.89 \pm 0.11) \times \log(M_{\rm star}) - (6.77 \pm 1.09) \quad (6)$$

the uncertainties on the coefficients (slope and constant) correspond to standard deviations, the global R.M.S. error is found equal to 0.16. This relation can be compared to other ones also obtained for UV selected galaxies from $z = 0$ to $z = 2$. Up to $z = 1$ the FUV rest-frame range

is well sampled with GALEX data. Buat *et al*. (2007) performed a statistical analysis of the GALEX and IRAS surveys and deduced volume corrected relations about far-IR and FUV properties of galaxies in the nearby universe. Here, we use their UV selected sample to calculate the average far-IR to FUV flux ratio per bin of stellar mass following the method explained in Buat *et al*. (2007). The amount of dust attenuation is then calculated by applying the relation of Buat *et al*. (2011a). The average values and the result of the linear regression fitted on them is reported in Fig. 5. Garn and Best (2010) obtained a relation between dust attenuation and stellar mass for SDSS galaxies based on the measure of the Balmer decrement, their relation is extrapolated at FUV wavelength using the Meurer *et al*. (2009) relation $A_{\rm FUV} = 1.68 A_{\rm H\alpha}$ and is also reported on Fig. 5. Note that this extrapolation is very crude given the large dispersion in the scatter plot between $A_{\rm FUV}$ and $A_{\rm H\alpha}$ and the uncertainty on the average value of $A_{\rm FUV}/A_{\rm H\alpha}$ (Bell and Kennicutt, 2001; Buat *et al*., 2002; Boselli *et al*., 2013). Buat *et al*. (2009) investigated UV selected galaxies from $z = 0$ to $z = 1$ and found a trend with $M_{\rm FUV}$ and no clear evolution with redshift of the $A_{\rm FUV}$-$M_{\rm star}$ scatter plot. We report their average relation corresponding to $\log(L_{\rm FUV}) = 10.2[L_\odot]$, representative of our current sample (see Buat *et al*. (2012) for more details). At $z = 2$ Sawicki (2012) built a FUV selected sample from the Ultra-deep Hubble field and found a relation between dust attenuation and stellar mass (estimated from the observed FUV luminosity), his relation is also reported in Fig. 5. The relation obtained in the present work for galaxies with redshift between 0.95 and 2.2 predicts slightly higher dust attenuation factors than the three other ones but remain consistent within the error bars with most of the relations considered in Fig. 5. The relation found at $z = 0$ by Buat *et al*. (2007) leads to lower dust attenuation for massive galaxies by $\sim$1 mag for $\log(M_{\rm star}) > 10.5[M_\odot]$ but their statistics for high mass galaxies was low. The Garn and Best relation based on larger statistics is found closer the other ones at higher z. We can conservatively conclude to a well defined relation between average dust attenuation and $M_{\rm star}$ for UV selected galaxies which does not show a significant evolution from $z = 0$ to $z = 2$.

The trend found with the FUV luminosity (i.e. a lower mean dust attenuation when $L_{\rm FUV}$ increases) is clearly visible in Fig. 5, upper panel. It might imply a modification of the mean relation as a function of the luminosity, the FUV luminosity also acting as a parameter in the variation of dust attenuation. A complete analysis of this relation per bin of FUV luminosity and stellar mass at different redshifts has still to be performed. The current samples are too small for such a study. Heinis *et al*. (in preparation) will analyze a much larger sample of galaxies in the COSMOS field based on stacked Herschel/SPIRE images to better constrain average dust attenuation factors.

Acknowledgments. This work is partially supported by the French National Agency for research (ANR-09-BLAN-0224). PACS has been developed by a consortium of institutes led by MPE (Germany) and including UVIE (Austria); KU Leuven, CSL, IMEC (Belgium); CEA, LAM (France); MPIA (Germany); INAFIFSI/OAA/OAP/OAT, LENS, SISSA (Italy); IAC (Spain). This development has been supported by the funding agencies BMVIT (Austria), ESA-PRODEX (Belgium), CEA/CNES (France), DLR (Germany), ASI/INAF (Italy), and CICYT/MCYT (Spain).

References

Bell, E. and R. C. Kennicutt, A comparison of ultraviolet imaging telescope far-ultraviolet and H? star formation rates, *Astrophys. J.*, **548**, 681–693, 2001.

Boselli *et al*., Integrated spectroscopy of the Herschel Reference Survey. The spectral line properties of a volume-limited, K-band selected sample of nearby galaxies, arXiv:1211.5262, 2013.

Buat *et al*., Star formation and dust extinction in nearby star-forming and starburst galaxies, *Astron. Astrophys.*, **383**, 801–812, 2002.

Buat *et al*., Local universe as seen in the far-infrared and far-ultraviolet: A global point of view of the local recent star formation, *Astrophys. J. Suppl. Ser.*, **173**, 404–414, 2007.

Buat *et al*., The infrared emission of ultraviolet-selected galaxies from z = 0 to z = 1, *Astron. Astrophys.*, **507**, 693, 2009.

Buat, V. *et al*., Spectral energy distributions of an AKARI-SDSS-GALEX sample of galaxies, *Astron. Astrophys.*, **529**, id.A22, 2011a.

Buat, V. *et al*., GOODS-Herschel: evidence of a UV extinction bump in galaxies at $z > 1$, *Astron. Astrophys.*, **533**, id.A93, 2011b.

Buat, V. *et al*., GOODS-Herschel: dust attenuation properties of UV selected high-redshift galaxies, *Astron. Astrophys.*, **545**, id.A141, 2012.

Burgarella, D., V. Buat, and J. Iglesias-Paramo, Star formation and dust attenuation properties in galaxies from a statistical ultraviolet-to-far-infrared analysis, *Mon. Not. R. Astron. Soc.*, **360**, 1413–1425, 2005.

Calzetti, D. *et al*., The dust content and opacity of actively star-forming galaxies, *Astrophys. J.*, **533**, 682–695, 2000.

Cardamone *et al*., The multiwavelength survey by Yale-Chile (MUSYC): Deep medium-band optical imaging and high-quality 32-band photometric redshifts in the ECDF-S, *Astrophys. J. Suppl.*, **189**, 270–285, 2010.

Conroy, C., D. Schiminovich, and M. R. Blanton, Dust attenuation in disk-dominated galaxies: Evidence for the 2175Ådust feature, *Astrophys. J.*, **718**, 184–198, 2010.

Draine, B. T., Scattering by interstellar dust grains. I. Optical and ultraviolet, *Astrophys. J.*, **598**, 1017–1025, 2003.

Elbaz, D. *et al*., GOODS-Herschel: an infrared main sequence for star-forming galaxies, *Astron. Astrophys.*, **533**, id.A119, 2011.

Fitzpatrick, E. L. and D. Massa, An analysis of the shapes of ultraviolet extinction curves. III—an atlas of ultraviolet extinction curves, *Astrophys. J. Suppl. Ser.*, **72**, 163–189, 1990.

Garn, T. and P. N. Best, Predicting dust extinction from the stellar mass of a galaxy, *Mon. Not. R. Astron. Soc.*, **409**, 421–432, 2010.

Gordon, K. *et al*., A quantitative comparison of the small Magellanic cloud, large Magellanic Cloud, and Milky Way ultraviolet to near-infrared extinction curves, *Astrophys. J.*, **594**, 279–293, 2003.

Heinis, *et al*., HerMES: unveiling obscured star formation—the far-infrared luminosity function of ultraviolet-selected galaxies at z = 1.5, arXiv:1211.4336.

Inoue, A. *et al*., Effects of dust scattering albedo and 2175-Åbump on ultraviolet colours of normal disc galaxies, *Mon. Not. R. Astron. Soc.*, **370**, 380–398, 2006.

Kroupa, P., *Mon. Not. R. Astron. Soc.*, **322**, 231–, 2001.

Meurer *et al*., Evidence for a nonuniform initial mass function in the local universe, *Astrophys. J.*, **695**, 765, 2009.

Noll, S. *et al*., Analysis of galaxy spectral energy distributions from far-UV to far-IR with CIGALE: studying a SINGS test sample, *Astron. Astrophys.*, **507**, 1793–1813, 2009.

Pilbratt, G. *et al*., Herschel Space Observatory. An ESA facility for far-infrared and submillimetre astronomy, *Astron. Astrophys.*, **518**, id.L1, 2010.

Sawicki, M., Stars, dust, and the growth of ultraviolet-selected sub-L galaxies at redshift $z \sim 2$, *Mon. Not. R. Astron. Soc.*, **421**, 2187–2205, 2012.

Wild, V. *et al*., Empirical determination of the shape of dust attenuation curves in star-forming galaxies, *Mon. Not. R. Astron. Soc.*, **417**, 1760–1786, 2011.

V. Buat (e-mail: veronique.buat@oamp.fr)